Transport in metals with electron-electron scattering

Werner W. Schulz
Institute of Physics and Astronomy, University of Aarhus, DK-8000 Aarhus C, Denmark
and Department of Physics, State University of New York at Stony Brook, Stony Brook, New York 11794-3800

Philip B. Allen
Department of Physics, State University of New York at Stony Brook, Stony Brook, New York 11794-3800
and Institut Romand de Recherche Numérique en Physique des Matériaux, CH-1015 Ecublens, Switzerland
(Received 10 April 1995; revised manuscript received 5 June 1995)

The problem of electron-electron scattering is solved using the Boltzmann equation and a special set of basis functions. This basis treats different scattering mechanisms on the same footing. Corrections beyond the level of Matthiessen's rule are easily generated. The resulting Boltzmann equation has a simple tridiagonal form for Coulomb scattering, and values of transport properties converge rapidly. Results for electrical and thermal conductivity, the Lorentz number, and the Hall coefficient are presented.

I. INTRODUCTION

A resistivity $\rho(T) \propto T^2$ is often regarded as the signature of a three-dimensional Fermi liquid. Actual metals usually display such behavior only in a regime of high purity and low temperature, which is difficult to attain experimentally.[1,2] However, "highly correlated" metals have larger Coulomb effects. Examples are the "heavy fermion" metals[3] where giant T^2 resistivities are seen, and the high-T_c superconductors where the normal state $\rho(T)$ and Hall coefficient R_H are anomalous. In particular, R_H, rather than being independent of T, often seems to vary[4] as $1/T$. Therefore, we offer in this paper some "exact" results for electron-electron scattering in "ordinary" metals. "Ordinary" means that the low-energy excitations are quasiparticles whose behavior is described by a Boltzmann equation[5] (BE). "Exact" means that the Boltzmann equation has been solved with good numerical convergence. In particular, we calculate the deviations from Mattheissen's rule and test the accuracy of the usual lowest-order solution. The results confirm earlier work of Smith and Wilkins[6] and of Lawrence and Wilkins.[7] Our main motivation was to see whether any interesting T dependence of R_H could arise by such a route. Our answer is negative; the Hall coefficient remains approximately independent of temperature even for strong inelastic electron-electron scattering.

A realistic calculation of $\rho(T)$ or $R_H(T)$ for a real metal is a daunting task. Assuming that the quasiparticle spectrum $\varepsilon_{\boldsymbol{k}}$ and scattering matrices are all known, one still has a Boltzmann equation that couples the distribution $F(\boldsymbol{k})$ for the electron state $\boldsymbol{k}$ near the Fermi surface (FS) to all other states $\boldsymbol{k}'$ near the Fermi surface. It is appropriate to separate the $\boldsymbol{k}$ variation into two types: (1) "angular" variation on the Fermi surface, and (2) "radial" variation with $\varepsilon_{\boldsymbol{k}}$ perpendicular to the Fermi surface. The first effect is highly nonuniversal, depending on the shape of the Fermi surface and other material-dependent details, while the second effect, especially for Coulomb and impurity scattering, is universal to good approximation. In the approximation that k_BT is small compared to electronic energy scales, effects (1) and (2) decouple from each other. Our work deals only with part (2). We neglect "anisotropy" effects coming from angular variations of the scattering matrices, and solve the remaining problem exactly.[8] However, our method permits the angular part of the problem to be restored if available information were to warrant it. We also ignore the "indirect" electron-electron interaction through exchange of virtual phonons,[9] which for many simpler metals gives the dominant part of the T^2 resistivity at low T. To include this effect would complicate the model but not the numerical algorithm used to solve the problem.

II. BOLTZMANN EQUATION

The linearized Boltzmann equation for electrons in a metal with a electrical field $\boldsymbol{E}$, a magnetic field $\boldsymbol{B}$, and thermal gradient ∇T is

$$\left(-\frac{\partial f}{\partial \varepsilon}\right)\left(q\boldsymbol{E}\cdot\boldsymbol{v}_{\boldsymbol{k}}-\frac{\varepsilon_{\boldsymbol{k}}}{T}\nabla T\cdot\boldsymbol{v}_{\boldsymbol{k}}\right)$$

$$=(\hat{Q}\Phi)(\boldsymbol{k})+\left(\frac{\partial f}{\partial \varepsilon}\right)\frac{q}{\hbar}\boldsymbol{B}\cdot[\boldsymbol{v}_{\boldsymbol{k}}\times\nabla_{\boldsymbol{k}}\Phi(\boldsymbol{k})], \quad (1)$$

where the energy $\varepsilon_{\boldsymbol{k}}$ is measured from the chemical potential μ, $\boldsymbol{v}_{\boldsymbol{k}}=\nabla_{\boldsymbol{k}}\varepsilon_{\boldsymbol{k}}/\hbar$, $\Phi(\boldsymbol{k})$ is the deviation of the distribution function F from equilibrium f, $F(\boldsymbol{k})=f(\varepsilon_{\boldsymbol{k}})-(\partial f/\partial\varepsilon)\,\Phi(\boldsymbol{k})$, and $(\hat{Q}\Phi)(\boldsymbol{k})$ is the linearized collision integral describing the scattering of electrons off electrons, impurities, or phonons. The magnetic field will be treated later.

The particular form of the driving terms and the associated currents led Allen[10] to define a biorthogonal set of basis functions (see Appendix A) indexed by $\{nJ\}$

where $n = 0, 1, 2, \ldots$, labels the behavior perpendicular to the Fermi surface and $J = x, y, z, x^2, \ldots$, labels the anisotropy of the Fermi surface. In this basis, the linearized Boltzmann equation reads

$$\left[qE_x\,\delta_{n0} - \frac{\pi k_B}{\sqrt{3}}\nabla_x T\,\delta_{n1}\right]\delta_{Jx} = \sum_{n'J'} Q_{nJ,n'J'}\,\Phi_{n'J'}\ , \tag{2}$$

with the electric field and the temperature gradient along the x axis. Electrical and thermal currents have a simple form

$$\begin{aligned} j_{ex} &= g\,q\sum_{\boldsymbol{k}} v_{\boldsymbol{k}x}\,\Phi(\boldsymbol{k})\left(-\frac{\partial f}{\partial\varepsilon_{\boldsymbol{k}}}\right) \\ &= g\,q\,\Phi_{0x} = \alpha_{00}E_x + \alpha_{01}\nabla_x T, \end{aligned} \tag{3a}$$

$$\begin{aligned} j_{Qx} &= g\sum_{\boldsymbol{k}} \varepsilon_{\boldsymbol{k}} v_{\boldsymbol{k}x}\,\Phi(\boldsymbol{k})\left(-\frac{\partial f}{\partial\varepsilon_{\boldsymbol{k}}}\right) \\ &= g\,\frac{\pi\,k_B T}{\sqrt{3}}\,\Phi_{1x} = \alpha_{10}E_x + \alpha_{11}\nabla_x T. \end{aligned} \tag{3b}$$

The spin degeneracy is denoted by $g\ (=2)$ and the charge of the electron by $q\ (=-e)$. The right-hand side of Eq. (3) defines the coefficients α_{ij}, which can be directly expressed in terms of the scattering matrix $\mathbf{Q}$,

$$\alpha_{00} = g\,q^2\,(\mathbf{Q}^{-1})_{0x,0x}, \tag{4a}$$

$$\alpha_{01} = -g\,q\,\frac{\pi\,k_B}{\sqrt{3}}\,(\mathbf{Q}^{-1})_{0x,1x}, \tag{4b}$$

$$\alpha_{10} = g\,q\,\frac{\pi\,k_B T}{\sqrt{3}}\,(\mathbf{Q}^{-1})_{1x,0x}, \tag{4c}$$

$$\alpha_{11} = -g\,\frac{\pi^2\,k_B^2 T}{3}\,(\mathbf{Q}^{-1})_{1x,1x}. \tag{4d}$$

The usual transport coefficients, electrical conductivity σ and thermal conductivity κ, are related to the α_{ij} through $\sigma = \alpha_{00}$, and $\kappa = -\alpha_{11} + \alpha_{10}\alpha_{00}^{-1}\alpha_{01}$.

III. ELECTRON-ELECTRON SCATTERING

The electron-phonon part of the scattering operator Q has been treated in the $\{nJ\}$ basis previously[10] and is ignored in this paper. Elastic impurity scattering is diagonal in the energy index n. Here we model it with an isotropic scattering time $\tau_{\rm imp}$,

$$Q^{\rm imp}_{nJ,n'J'} = \frac{g}{(n/m)_{\rm eff}}\,\frac{1}{\tau_{\rm imp}}\,\delta_{nn'}\,\delta_{JJ'}. \tag{5}$$

For inelastic electron-electron (Coulomb) scattering, $\hat{Q}^C\Phi$ is

$$\begin{aligned} (\hat{Q}^C\Phi)(\boldsymbol{k}_1) = {}& \frac{2\pi}{k_B T\,\hbar} \\ & \times\sum_{2,3,4} |V(1,2,3,4)|^2\delta(\varepsilon_1+\varepsilon_2-\varepsilon_3-\varepsilon_4) \\ & \times\{f(\varepsilon_1)\,f(\varepsilon_2)\,[1-f(\varepsilon_3)]\,[1-f(\varepsilon_4)]\} \\ & \times[\Phi(\boldsymbol{k}_3)+\Phi(\boldsymbol{k}_4)-\Phi(\boldsymbol{k}_1)-\Phi(\boldsymbol{k}_2)], \end{aligned} \tag{6}$$

where $1,2$ and $3,4$ denote the electrons scattered in and out, respectively. $|V(1,2,3,4)|^2$ is the matrix element of the equilibrium transition probability. The detailed analysis of Q^C and its matrix representation in the $\{nJ\}$ basis is given in Appendix B. Assuming $k_B T \ll \varepsilon_F$, the scattering matrix Q^C is

$$Q^C_{nJ,n'J'} = \frac{4\pi^3\,k_B^2 T^2}{\hbar}\,\frac{gN_\uparrow(0)}{(n/m)_{\rm eff}}\,\sum_{i=1}^{3}\gamma_i(JJ')\,R_i(nn'), \tag{7}$$

where the $\gamma_i(JJ')$ are material-dependent parameters, $N_\uparrow(0)$ is the density of states at the Fermi level, and

$$(n/m)_{\rm eff} = \sum_{\boldsymbol{k}}\delta(\varepsilon_{\boldsymbol{k}})v^2_{\boldsymbol{k}x} = gN_\uparrow(0)v^2(0)\ .$$

The important inelastic scattering effects are all included in the universal numbers $R_i(nn')$. Since $R_i(nn')$ vanishes if $n+n'$ is odd, the Boltzmann equation splits into two uncoupled equations,

$$q\,E_x\,\delta_{n0}\delta_{Jx} = \sum_{n'J'}^{n'\,\rm even} Q^{C,E}_{nJ,n'J'}\,\Phi_{n'J'}, \tag{8a}$$

$$-\frac{\pi k_B}{\sqrt{3}}\nabla_x T\,\delta_{n1}\delta_{Jx} = \sum_{n'J'}^{n'\,\rm odd} Q^{C,T}_{nJ,n'J'}\,\Phi_{n'J'}, \tag{8b}$$

where E and T designate the submatrices of even and odd n, respectively. We despair of being able to solve the anisotropy problem because to treat it properly requires a microscopic theory of scattering so that we can compute the many material-dependent parameters $\gamma_i(JJ')$. We are far from having this ability except in the simplest metals. Fortunately, it is often safe to assume that $\gamma_i(xx)$ is much bigger than any off-diagonal $\gamma_i(xJ')$. We keep only the $J = J' = x$ component of $Q_{nJ,n'J'}$ and have

$$\begin{aligned} Q^{C,E}_{nx,n'x} = {}& \frac{4\pi^3\,k_B^2 T^2}{\hbar}\,\frac{gN_\uparrow(0)}{(n/m)_{\rm eff}} \\ & \times\left[\gamma_1\,R_1(nn') + (\gamma_2+\gamma_3)\,R_2(nn')\right], \end{aligned} \tag{9a}$$

$$\begin{aligned} Q^{C,T}_{nx,n'x} = {}& \frac{4\pi^3\,k_B^2 T^2}{\hbar}\,\frac{gN_\uparrow(0)}{(n/m)_{\rm eff}} \\ & \times\left[\gamma_1\,R_1(nn') + (\gamma_2-\gamma_3)\,R_2(nn')\right], \end{aligned} \tag{9b}$$

where γ_i is a short notation for $\gamma_i(xx)$. For the sake of simplicity, we combine the different constants into a time $\tau_c(T)$,

$$\tau_c^{-1} = \frac{4\pi^3\,k_B^2 T^2}{3\hbar}\,N_\uparrow(0)\gamma_1, \tag{10}$$

and two FS parameters,[7] $\Delta = (\gamma_1+\gamma_2+\gamma_3)/\gamma_1$ and $\langle\cos\theta\rangle = \gamma_2/\gamma_1$, where γ_1 is a measure of the strength of Coulomb scattering on the Fermi surface, Δ measures the relative amount of umklapp scattering, and $\langle\cos\theta\rangle$ is a weighted FS average of the angle between the two incoming electrons (see Appendix B). A temperature T_0 is defined at the crossover from impurity to Coulomb scattering via $\tau_c(T_0) = \tau_{\rm imp}$,

$$\frac{T^2}{T_0^2} = t^2 = \frac{4\pi^3 k_B^2 T^2 N_\uparrow(0)}{3\hbar}\,\gamma_1\tau_{\rm imp} = \frac{\tau_{\rm imp}}{\tau_c}. \quad (11)$$

The scattering matrices, including the impurity terms, can now be written as

$$Q^E_{nx,n'x} = \frac{g}{(n/m)_{\rm eff}\,\tau_{\rm imp}} \times\{\delta_{nn'} + 3t^2[R_1(nn') - (1-\Delta)R_2(nn')]\}, \quad (12a)$$

$$Q^T_{nx,n'x} = \frac{g}{(n/m)_{\rm eff}\,\tau_{\rm imp}}\{\delta_{nn'} + 3t^2[R_1(nn') + (1 + 2\langle\cos\theta\rangle - \Delta)\,R_2(nn')]\}. \quad (12b)$$

In both cases, $Q = Q^{\rm imp} + Q^C$ is a symmetric tridiagonal matrix with the welcome side effect that the inversion of Q is a $O(N)$ process. The electrical and thermal conductivities can be expressed in the scaled temperature $t = T/T_0$,

$$\sigma(t,\Delta) = \left[q^2(n/m)_{\rm eff}\,\tau_{\rm imp}\right], \quad (13)$$

$$\tilde\sigma(t,\Delta) = \sigma_0\,\tilde\sigma(t,\Delta),$$

$$\kappa(t,\Delta,\theta) = \left[\frac{\pi^2}{3}k_B^2 T_0\,(n/m)_{\rm eff}\,\tau_{\rm imp}\right], \quad (14)$$

$$t\,\tilde\kappa(t,\Delta,\theta) = \kappa_0\,t\,\tilde\kappa(t,\Delta,\theta),$$

where σ_0 and $\kappa_0 t$ are the conductivities for impurity scattering only. The effect of adding Coulomb scattering is described by the dimensionless functions $\tilde\sigma(t,\Delta)$ and $\tilde\kappa(t,\Delta,\theta)$.

The Boltzmann equation obeys a variational principle,[11] and usually the lowest-order (LO) case, i.e., $(nJ) = (0x)$ or $(1x)$, is already a good approximation,

$$\tilde\sigma_{\rm LO} = \left[1 + t^2\Delta\right]^{-1}, \quad (15)$$

$$\tilde\kappa_{\rm LO} = \left[1 + \frac{3}{5}t^2\,(2 - 2\langle\cos\theta\rangle + \Delta)\right]^{-1}, \quad (16)$$

with the Lorentz number $L_{\rm LO}$

$$L_{\rm LO}(t,\Delta,\theta) = L_0\,\frac{1 + t^2\Delta}{1 + t^2\,(6/5 - 6/5\langle\cos\theta\rangle + 3/5\Delta)}, \quad (17)$$

where L_0 is the free-electron result, $L_0 = \pi^2 k_B^2/3\,q^2$. In the limit of impurity scattering ($t \to 0$), $L_{\rm LO} \to L_0$. The LO result also provides lower bounds for the FS parameters Δ and $\langle\cos\theta\rangle$,

$$\Delta > 0, \quad (18a)$$

$$2 - 2\langle\cos\theta\rangle + \Delta > 0. \quad (18b)$$

Both bounds are always fulfilled since $\Delta \propto \langle \boldsymbol{v}_1 + \boldsymbol{v}_2 - \boldsymbol{v}_3 - \boldsymbol{v}_4\rangle^2$ and the definition of θ ensures $1 - \langle\cos\theta\rangle \geq 0$.

The overall behavior of the transport coefficients follows the well-known limiting cases, i.e., in the regime of impurity scattering (low t), $\sigma = \sigma_0$ and $\kappa = \kappa_0 t$, while for Coulomb scattering (large t), $\sigma \propto t^{-2}$ and $\kappa \propto t^{-1}$ with the crossover at $t \approx 1$. In both limits the Lorentz number is a constant, but the coefficients of σ, κ, and L are strongly dependent on the magnitude of Δ and $\langle\cos\theta\rangle$; for L see Fig. 1. The dependence on Δ is easily understood. The resisitivity of metal is increased if it is a strong umklapp scatterer as a large amount of momentum is transferred to the crystal lattice. The changes in electrical and thermal conductivity are roughly proportional to $1/\Delta$. Similarly, a large angle θ leads to a large loss of momentum and, hence, to an increase in thermal resistivity. The Lorentz number $L = \kappa/T\sigma$ shows strong deviations from the Wiedemann-Franz law $L = L_0$ in Fig. 1 and has become an important tool to extract information about electron-electron scattering at high temperatures.[1] We find that over the whole temperature range, the exact Lorentz number L is very well approximated by the fit

$$L(t,\Delta,\theta) = L_0\,\frac{1 + (at)^2\Delta}{1 + (at)^2(0.98 - 0.88\langle\cos\theta\rangle + 0.56\Delta)}, \quad (19)$$

with $a = 1.06$. It must be remembered that the Wiedemann-Franz law is an empirical law and does not hold everywhere, e.g., the Lorentz number vanishes in the limit of pure Coulomb scattering, ($t = \infty$) and $\Delta \to 0$. For electron-phonon scattering the Lorentz number is usually close to its classical value L_0 except at very low temperatures.[10]

Although the LO approximation is excellent at low t, its quality decreases at higher temperatures. Figures 2 – 4 show the ratio of the exact ($N \to \infty$) over the LO result

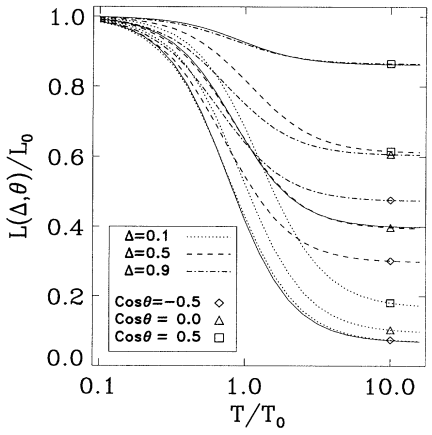

FIG. 1. Lorentz number L vs temperature T/T_0. L is normalized to the $T = 0$ limit, L_0. The line styles and symbols are explained in the inset. The solid lines are plots of the fit Eq. (19) for a few selected parameters.

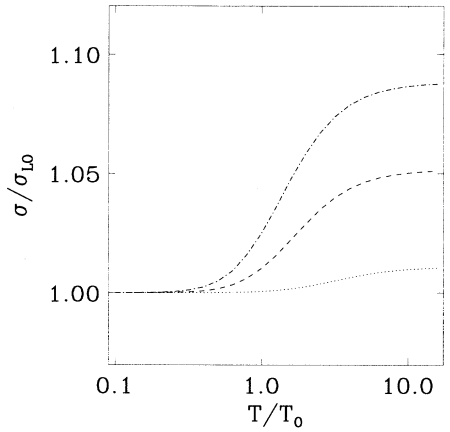

FIG. 2. Ratio of electrical conductivity σ and the lowest-order result as a function of temperature T/T_0. Figure 1 explains the line styles.

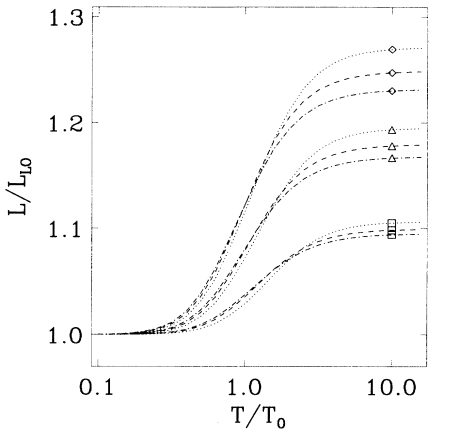

FIG. 4. Ratio of Lorentz number L and the lowest-order result as a function of temperature T/T_0. Figure 1 explains the line styles.

as a function of the temperature t. The thermal conductivity in particular shows more than 20% deviation for reasonable choices of the parameters Δ and $\langle\cos\theta\rangle$. The LO approximation is the better the smaller the angle θ and the amount of umklapp scattering as measured by Δ's.

An important feature of our choice of basis functions is the fast convergence of the transport properties; as an example we show in Fig. 5 results for the thermal conductivity κ for several choices of temperature $t = T/T_0$ and Δ. A few basis functions ($N \approx 4$) are sufficient to be within 1% of the exact result obtained by a $1/N$ extrapolation. The convergence happens fast in spite of a slow convergence of the distribution function $\Phi(\boldsymbol{k})$ itself.

According to Eq. (8a), the expansion coefficients $\Phi_{n\boldsymbol{x}}$ of $\Phi(\boldsymbol{k})$ are solutions of the normalized equation

$$\delta_{n0} = \sum_{n' \text{ even}} \left[\delta_{nn'} + 3t^2 R(nn')\right] \Phi_{n'\boldsymbol{x}}(t), \tag{20}$$

$$\Phi(\boldsymbol{k}) = qE_{\boldsymbol{x}} v_{\boldsymbol{kx}} \tau_{\text{imp}} \sum_n \Phi_{n\boldsymbol{x}} \sigma_n(\varepsilon). \tag{21}$$

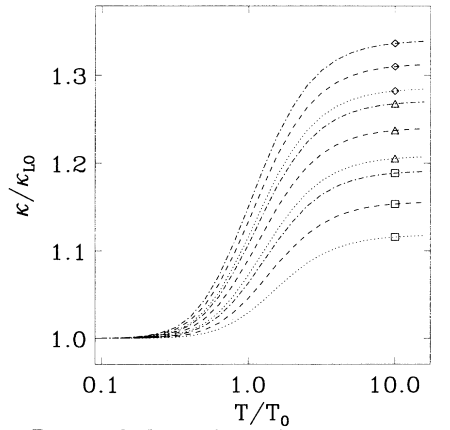

FIG. 3. Ratio of thermal conductivity κ and the lowest-order result as a function of temperature T/T_0. Figure 1 explains the line styles.

The total distribution function $F(\boldsymbol{k})$ is a shifted Fermi function,

$$F(\boldsymbol{k}) = f(\varepsilon_{\boldsymbol{k}}) - \left(\frac{\partial f}{\partial \varepsilon}\right) \Phi(\boldsymbol{k}) \tag{22}$$

$$\approx f\left[\varepsilon_{\boldsymbol{k}} - qE_{\boldsymbol{x}} v_{\boldsymbol{kx}} \tau(\varepsilon, t)\right], \tag{23}$$

for a slowly varying "relaxation time" (RT) $\tau(\varepsilon, t) = \tau_{\text{imp}} \sum_n \Phi_{n\boldsymbol{x}}(t)\, \sigma_n(\varepsilon)$. Although we use the name relaxation time, note that this RT is obtained from an exact solution of the linear Boltzmann equation Eq. (2) and *not* from the usual relaxation time ansatz $F(\boldsymbol{k}) = f(\varepsilon_{\boldsymbol{k}} - qE_x v_{\boldsymbol{kx}} \tau)$. Figure 6 shows the slow convergence of the partial sums $\tau_n = \sum_i^n \Phi_i^n(t) \sigma_i(\varepsilon)$ in the regime of Coulomb scattering. The convergence is similar in the case of a thermal gradient.

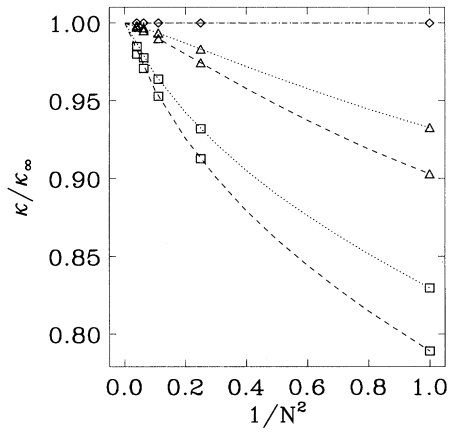

FIG. 5. Convergence of conductivity $\kappa(t, \Delta, \theta)$ for different number N of basis functions. Each κ is normalized with the exact result for $N = \infty$. The convergence is shown for several values of temperature $t = T/T_0$ ($\diamond$, $t = 0.1$; $\triangle$, $t = 1.0$; $\square$, $t = 10.0$) and Δ (dotted line, $\Delta = 0.1$; dashed line, $\Delta = 0.9$).

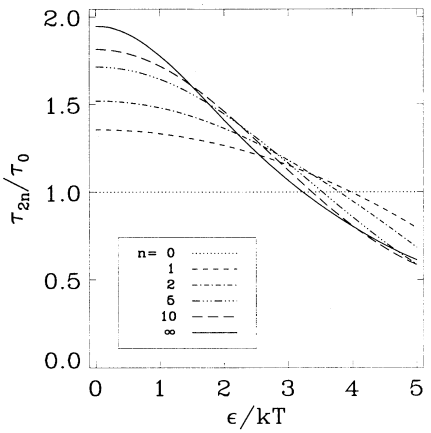

FIG. 6. Convergence of the electrical relaxation time $\tau(\varepsilon)$ as defined in the text. The parameters are $T/T_0 = 10.0$ and $\Delta = 0.9$.

IV. MAGNETIC FIELD AND HALL COEFFICIENT

A magnetic field $\boldsymbol{B}$ can provide additional information about quasiparticles at the FS. The weak-field Hall coefficient $R_H = \sigma_{xy}/\sigma_{xx}\,\sigma_{yy}B$ is a commonly measured transport coefficient. In the following we assume that only a single connected FS is present. The magnetic field $\boldsymbol{B}$ is included in the Boltzmann equation (1) through

$$(\hat{A}\Phi)(\boldsymbol{k}) = \left(\frac{\partial f}{\partial \varepsilon}\right) \frac{q}{\hbar}\epsilon_{\alpha\beta\gamma}B_\alpha\, v_{\beta\boldsymbol{k}}\nabla_\gamma\Phi(\boldsymbol{k}), \tag{24}$$

where $\epsilon_{\alpha\beta\gamma}$ is the Levi-Civita antisymmetric tensor and summation over its indices is implied. Formally similar to the electron-electron scattering term, the magnetic field adds to the right-hand side of Eq. (2) a term[12] $\sum_{n'J'} A_{nJ,n'J'}\,\Phi_{n'J'}$, where

$$A_{nJ,n'J'} = -\frac{q}{\hbar}\epsilon_{\alpha\beta\gamma}\mathbf{B}_\alpha \int_{-\infty}^{\infty} d\varepsilon \left(-\frac{\partial f}{\partial \varepsilon}\right) \sigma_n(\varepsilon)\,\sigma_{n'}(\varepsilon) \times \left[N_\uparrow(\varepsilon)\,v(\varepsilon)\right]^{-2} \times \sum_{\boldsymbol{k}} \delta(\varepsilon - \varepsilon_{\boldsymbol{k}})\; v_{\boldsymbol{k}\beta}\; F_J(\boldsymbol{k})\; \nabla_\gamma F_{J'}(\boldsymbol{k}). \tag{25}$$

The ε-dependent functions are not affected by the gradient because $\boldsymbol{v_k} \times \nabla h(\varepsilon_{\boldsymbol{k}})$ vanishes for any function $h(\varepsilon_{\boldsymbol{k}})$. The radial integral is approximately diagonal in (nn') if the density of states $N_\uparrow(\varepsilon)$ and the velocity $v(\varepsilon)$ vary slowly around the Fermi level,

$$A_{ny,n'x} = \frac{g}{(n/m)_{\text{eff}}}\,\Omega_c\,\delta_{nn'}\,, \tag{26}$$

where only $J = x, y$ is kept, following our approximations in the previous section. The direction of the magnetic field is chosen along the z axis, and Ω_c is the FS-averaged cyclotron frequency

$$\Omega_c = \frac{q\,B_z}{\hbar}\sum_{\boldsymbol{k}} \delta(\varepsilon_{\boldsymbol{k}})\, v_{x\boldsymbol{k}}\left[v_{x\boldsymbol{k}}\,\nabla_y v_{y\boldsymbol{k}} - v_{y\boldsymbol{k}}\,\nabla_x v_{y\boldsymbol{k}}\right] \Big/ \sum_{\boldsymbol{k}} \delta(\varepsilon_{\boldsymbol{k}})\, v_{x\boldsymbol{k}}^2. \tag{27}$$

In the free-electron case, Eq. (27) reduces to $\Omega_c = qB_z/m$. In the weak-field limit, the scattering operator is expanded to first order in A, $(Q + A)^{-1} = Q^{-1} - Q^{-1}AQ^{-1} + \cdots$, and we get

$$\sigma_{xy} = gq^2\,(Q^{-1}AQ^{-1})_{0y,0x}. \tag{28}$$

The exact answer in Boltzmann theory for the Hall coefficient is

$$R_H = \frac{A_{0x,0y}}{gq^2\,B_z}\,\frac{(Q^{-1}AQ^{-1})_{0x,0y}}{(Q^{-1})_{0x,0x}\;A_{0x,0y}\;(Q^{-1})_{0y,0y}}, \tag{29}$$

where the first factor is the LO result and determined by the shape of the FS only, and the second factor is often close to one for all temperatures. This means that the Hall coefficient is not sensitive to the nature of the collision processes described by Q. In the approximation of Eq. (26), the Hall coefficient reduces to

$$R_H = \frac{\Omega_c/B_z}{q^2(n/m)_{\text{eff}}}\,\frac{(Q^{-2})_{0x,0x}}{(Q^{-1})^2_{0x,0x}}. \tag{30}$$

In this approximation it is easy to see that the Hall coefficient has at most a weak temperature dependence and that it cannot change sign. The correction factor can have different values in different scattering limits, leading to a weak T dependence in intermediate regions. The LO expression for the Hall coefficient, $R_H = \Omega_c/\left[B_z q^2 (n/m)_{\text{eff}}\right]$, is independent of T, and shows only small deviations of a few percent from the result of Eq. (30) (see Fig. 7).

Any strong temperature dependence of the Hall coefficient must come from a rapid variation of the electronic properties around the FS, i.e., a variation on the scale

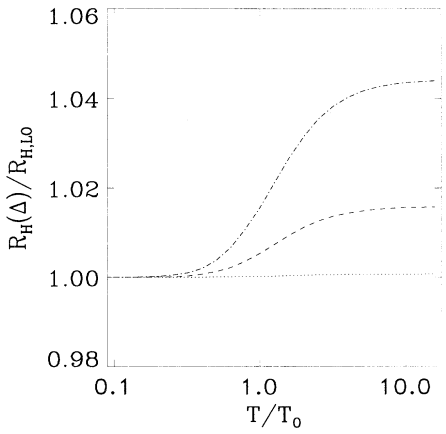

FIG. 7. Ratio of the Hall coefficient R_H to the lowest-order approximation as a function of T/T_0 and Δ. The values of Δ are the same as in Fig. 1.

k_BT, or from the presence of disconnected FS where the relative weight of scattering from electron and holelike FS is changed with increasing temperature. This has been observed in NbO,[13] where even a change of sign in R_H is seen.

V. CONCLUSION

Our formalism allows us to treat different interactions (Coulomb, impurity, and electron-phonon) on the same footing. The resulting matrix formulation of the BE includes the deviations from Matthiessen's rule with little extra effort. Magnetic effects are easily included. Although the basis function set is not chosen for a particular scattering mechanism convergence to the exact results is rapid.

We found that the Hall coefficient shows at most a weak dependence on the underlying microscopic scattering mechanism and temperature but is determined by the shape and curvature of the Fermi surface. The behavior found in the high-T_c cuprates[4] and recently in the C_{60} compounds[14] cannot be explained within the simple approximations we have used here.

While more difficult than in the electron-phonon case, it is possible to extract the strength of the Coulomb interaction at the Fermi level from the experimental data, especially if low- and high-temperature data are available. The procedure is similar to that used in the case of electron-phonon coupling constant.[15] The largest hurdle at present in applying this approach is the difficulty of measuring Coulomb scattering in many metals.[2]

ACKNOWLEDGMENTS

We would like to thank M. Sotiropoulos for his help. We thank R. Askey for providing us with references about the orthogonal polynomials of Appendix A. This work was supported in part by NSF Grant No. DMR-9417755, by a grant from the Danish Research Council, Grant No. 9401617, and in part by the Division of Materials Sciences, U.S. Department of Energy, under Contract No. DE-AC02-76CH00016.

APPENDIX A: ORTHONORMAL FUNCTIONS IN TRANSPORT THEORY

In order to cast the Bloch-Boltzmann equation into matrix form, it is very helpful to introduce a special set of orthonormal functions. The nature of the problem suggests that the energy (or radial) coordinates and the angular coordinates (i.e., coordinates on a constant energy surface) are separated. The energies are measured from the chemical potential.

We choose[10] the radial basis functions $\sigma_n(\varepsilon)$ to be polynomials defined through

$$\int_{-\infty}^{\infty} d\varepsilon \left(-\frac{\partial f(\beta\varepsilon)}{\partial\varepsilon}\right) \sigma_n(\varepsilon)\sigma_m(\varepsilon) = \delta_{nm}, \tag{A1}$$

where $f(x) = 1/[\exp(x)+1]$.

The recurrence relation for these polynomials can be written more easily by introducing a new function ζ through $\sigma_n(\varepsilon) = \sqrt{2n+1}\,\zeta_n(\beta\varepsilon/2\pi)$:

$$\pi \int_{-\infty}^{\infty} dx \frac{\zeta_n(x)\,\zeta_m(x)}{\cosh^2(\pi x)} = \frac{2}{2n+1}\delta_{nm}, \tag{A2a}$$

with $\zeta_0(x) = 1$ and $\zeta_1(x) = 2x$. These polynomials are a special case of a recently discovered class of orthogonal polynomials, the so-called continuous Hahn polynomials,[16] which are defined by

$$\int_{-\infty}^{\infty} dx\; P_n(x)\,P_m(x)\; w(x)$$

$$= \frac{\Gamma(n+a+c)\Gamma(n+a+d)\Gamma(n+b+c)\Gamma(n+b+d)}{(2n+a+b+c+d-1)\Gamma(n+a+b+c+d-1)} \times\delta_{nm}, \tag{A3a}$$

$$w(x) = \frac{1}{2\pi}\Gamma(a+ix)\Gamma(b+ix)\Gamma(c-ix)\Gamma(d-ix). \tag{A3b}$$

The polynomial $P_n(x)$ can be expressed as a hypergeometric function

$$P_n(x) = i^n \frac{(a+c)_n(a+d)_n}{n!} \times {}_3F_2\left(\begin{matrix}-n, n+a+b+c+d-1, a-ix \\ a+c, a+d\end{matrix}; 1\right), \tag{A3c}$$

where $(a)_k = a(a+1)\cdots(a+k-1)$. The orthogonal polynomials defined above correspond to the special case $a=b=c=d=1/2$ with the recursion relation[17]

$$n^2\,\zeta_n(x) = 2(2n-1)\,x\,\zeta_{n-1}(x) - (n-1)^2\,\zeta_{n-2}(x). \tag{A4}$$

The angular basis $F_J(\boldsymbol{k})$ is defined through

$$\frac{\sum_{\boldsymbol{k}} \delta(\varepsilon-\varepsilon_{\boldsymbol{k}})\,F_J(\boldsymbol{k})\,F_{J'}(\boldsymbol{k})}{\sum_{\boldsymbol{k}}\delta(\varepsilon-\varepsilon_{\boldsymbol{k}})} = \delta_{JJ'}. \tag{A5}$$

Further details about the angular basis can be found in Ref. 10.

Our basis functions are defined as the biorthogonal set

$$\chi_{nJ}(\boldsymbol{k}) = \sigma_n(\varepsilon_{\boldsymbol{k}})\,F_J(\boldsymbol{k})\,/N_\uparrow(\varepsilon_{\boldsymbol{k}})\,v(\varepsilon_{\boldsymbol{k}}), \tag{A6a}$$

$$\xi_{nJ}(\boldsymbol{k}) = \sigma_n(\varepsilon_{\boldsymbol{k}})\,F_J(\boldsymbol{k})\,v(\varepsilon_{\boldsymbol{k}})\left(-\frac{\partial f}{\partial\varepsilon_{\boldsymbol{k}}}\right), \tag{A6b}$$

with

$$\sum_{\boldsymbol{k}} \chi_{nJ}(\boldsymbol{k})\xi_{n'J'}(\boldsymbol{k}) = \int_{-\infty}^{\infty} d\varepsilon\,\sigma_n(\varepsilon)\sigma_{n'}(\varepsilon)\left(-\frac{\partial f}{\partial\varepsilon}\right) \times\left\{\sum_{\boldsymbol{k}}\delta(\varepsilon-\varepsilon_{\boldsymbol{k}})\,F_J(\boldsymbol{k})\,F_{J'}(\boldsymbol{k})\right\}\Big/ N_\uparrow(\varepsilon) = \delta_{nm}\,\delta_{JJ'}. \tag{A7}$$

Any function can now be expressed in terms of these basis functions, for example,

$$\phi(\boldsymbol{k}) = \sum_{nJ} \phi_{nJ}\, \chi_{nJ}(\boldsymbol{k}), \tag{A8a}$$

$$\phi_{nJ} = \sum_{\boldsymbol{k}} \phi(\boldsymbol{k})\, \xi_{nJ}(\boldsymbol{k}). \tag{A8b}$$

Similarly, any operator can be represented through its matrix elements.

APPENDIX B: SCATTERING MATRIX

We present the detailed calculation of the scattering matrix Q^C of Eq. (1) and justify the approximations that lead to the factorized form of Q^C in Eq. (7). After linearizing, the collision integral is a linear functional of $\Phi(\boldsymbol{k})$:

$$\left(\frac{\partial F(\boldsymbol{k})}{\partial t}\right)_{\text{coll}} = (\hat{Q}\Phi)(\boldsymbol{k}) \tag{B1}$$

$$= \frac{2\pi\beta}{\hbar} \sum |V(\boldsymbol{k},\boldsymbol{p};\boldsymbol{q})|^2 \delta_{\boldsymbol{G}}(\boldsymbol{k}+\boldsymbol{p}-\boldsymbol{k}'-\boldsymbol{p}') \times \{\Phi(\boldsymbol{k})+\Phi(\boldsymbol{p})-\Phi(\boldsymbol{k}')-\Phi(\boldsymbol{p}')\} \times f_{\boldsymbol{k}}\, f_{\boldsymbol{p}}\, (1-f_{\boldsymbol{k}'})\, (1-f_{\boldsymbol{p}'}) \times \delta(\varepsilon_{\boldsymbol{k}}+\varepsilon_{\boldsymbol{p}}-\varepsilon_{\boldsymbol{k}'}-\varepsilon_{\boldsymbol{p}'}), \tag{B2}$$

where $\boldsymbol{k},\boldsymbol{p}$ and $\boldsymbol{k}',\boldsymbol{p}'$ are the momenta of the incoming and outgoing electrons, respectively, $V(\boldsymbol{k},\boldsymbol{p};\boldsymbol{q})$ is the two-particle scattering potential with momentum transfer $\boldsymbol{q} = \boldsymbol{k} - \boldsymbol{k}'$. The notation $\delta_{\boldsymbol{G}}$ describes crystal momentum conservation for a reciprocal lattice vector $\boldsymbol{G}$, including normal ($\boldsymbol{G} = 0$) and umklapp processes ($\boldsymbol{G} \neq 0$), and $\boldsymbol{k}, \ldots,$ are vectors of the first Brillouin zone. In the following the sum over the $\boldsymbol{G}$ vectors is implied. We manipulate the collision integral by expressing Φ in the basis $\chi_{n'J'}$,

$$\sum_{\boldsymbol{k}} \chi_{nJ}(\boldsymbol{k})\, (\hat{Q}\Phi)(\boldsymbol{k}) = \sum_{n'J'} Q^C_{nJ,n'J'} \Phi_{n'J'}, \tag{B3}$$

where

$$Q^C_{nJ,n'J'} = \frac{2\pi\beta}{\hbar} \sum_{\boldsymbol{k},\boldsymbol{p};\boldsymbol{q}} |V(\boldsymbol{k},\boldsymbol{p};\boldsymbol{q})|^2 \delta(\varepsilon_{\boldsymbol{k}}+\varepsilon_{\boldsymbol{p}}-\varepsilon_{\boldsymbol{k}'}-\varepsilon_{\boldsymbol{p}'}) \times \chi_{nJ}(\boldsymbol{k})\, [\chi_{n'J'}(\boldsymbol{k}) + \chi_{n'J'}(\boldsymbol{p}) - \chi_{n'J'}(\boldsymbol{k}') - \chi_{n'J'}(\boldsymbol{p}')]\, f_{\boldsymbol{k}}\, f_{\boldsymbol{p}}\, (1-f_{\boldsymbol{k}'})\, (1-f_{\boldsymbol{p}'}). \tag{B4}$$

We use the form of our biorthogonal basis (Appendix A) to separate energy and angular variables. We introduce the more convenient notation $\chi_{nJ}(\boldsymbol{k}) = (n\varepsilon) \times F_J(\boldsymbol{k})$. The factorization of Eq. (B4) is easily done by inserting the identities $1 = \int d\varepsilon_1 \delta(\varepsilon_1 - \varepsilon_{\boldsymbol{k}})$, etc. After we reordered and relabeled the dummy variables of the angular and radial terms, the matrix Q^C can be expressed through purely energy-dependent terms and dimensionless spectral functions $\gamma_i(JJ';\varepsilon,\varepsilon,\varepsilon,\varepsilon)$, $(i = 1,2,3)$,

$$Q^C_{nJ,n'J'} = \frac{2\pi\beta}{\hbar} N_\uparrow(0)^2 \int d\varepsilon_1\, d\varepsilon_2\, d\varepsilon_3\, d\varepsilon_4\, \delta(\varepsilon_1+\varepsilon_2-\varepsilon_3-\varepsilon_4) f(\varepsilon_1) f(\varepsilon_2)\, [1-f(\varepsilon_3)][1-f(\varepsilon_4)] \times [(n\varepsilon_1)(n'\varepsilon_1)\gamma_1(JJ';\varepsilon_1,\varepsilon_2,\varepsilon_3,\varepsilon_4) + (n\varepsilon_1)(n'\varepsilon_2)\gamma_2(JJ';\varepsilon_1,\varepsilon_2,\varepsilon_3,\varepsilon_4) + (n\varepsilon_1)(n'\varepsilon_3)\gamma_3(JJ';\varepsilon_1,\varepsilon_2,\varepsilon_3,\varepsilon_4)], \tag{B5}$$

with

$$\gamma_1(JJ';\varepsilon_1,\varepsilon_2,\varepsilon_3,\varepsilon_4) = \langle F_J(\boldsymbol{k})\, F_{J'}(\boldsymbol{k})\rangle, \tag{B6a}$$

$$\gamma_2(JJ';\varepsilon_1,\varepsilon_2,\varepsilon_3,\varepsilon_4) = \langle F_J(\boldsymbol{k})\, F_{J'}(\boldsymbol{p})\rangle, \tag{B6b}$$

$$\gamma_3(JJ';\varepsilon_1,\varepsilon_2,\varepsilon_3,\varepsilon_4) = -2\,\langle F_J(\boldsymbol{k})\, F_{J'}(\boldsymbol{k}')\rangle, \tag{B6c}$$

where the brackets denote the weighted FS integral

$$\langle Y\rangle = \frac{1}{N_\uparrow(0)^2} \sum_{\boldsymbol{k},\boldsymbol{p};\boldsymbol{q}} |V(\boldsymbol{k},\boldsymbol{p};\boldsymbol{q})|^2\, Y \delta(\varepsilon_1-\varepsilon_{\boldsymbol{k}}) \times \delta(\varepsilon_2-\varepsilon_{\boldsymbol{p}})\delta(\varepsilon_3-\varepsilon_{\boldsymbol{k}'})\delta(\varepsilon_4-\varepsilon_{\boldsymbol{p}'}). \tag{B6d}$$

So far we have made no approximations beyond those contained in the Boltzmann equation itself. By keeping only the leading term in a k_BT/ε_F-type expansion, we get a simpler form that allows more insight. Two energy scales are involved in our problem: the temperature scale k_BT and a scale over which the density of states $N_\uparrow(\varepsilon)$, $v(\varepsilon)$, and other electronic properties vary, usually on the order of 0.1–5.0 eV $\gg k_BT$. The product of the Fermi functions is sharply peaked around the chemical potential due to energy conservation with a width $\propto k_BT$. In most practical cases, k_BT is small compared to the energy scale ε_F on which electronic properties like $N_\uparrow(\varepsilon)$ are varying. Then we can approximate $\gamma_i(JJ';\varepsilon_1,\varepsilon_2,\varepsilon_3,\varepsilon_4)$ by $\gamma_i(JJ';0000) = \gamma_i(JJ')$, and the spectral functions become FS averaged measures of the strength of the screened e-e interaction.

At the same time we replace $(n\varepsilon)$ by $\sigma_n(\varepsilon)/N_\uparrow(0)v(0)$. We can simplify Eq. (B5) further by using $1 - f(\varepsilon) = f(-\varepsilon)$. Since σ_n is either even or odd, this change of sign is easily accounted for. This allows us to write

$$Q^C_{nJ,n'J'} = \frac{4\pi^3\, gN_\uparrow(0)}{\hbar\beta^2\, (n/m)_{\text{eff}}} \sum_{i=1}^{3} \gamma_i(JJ')\, R_i(nn'), \tag{B7}$$

where we used $N_\uparrow(0)v^2(0) = (n/m)_{\rm eff}/g$ and the dimensionless energy integrals $R_i(nn')$ have the form

$$R_1(nn') = \frac{\beta^3}{2\pi^2}\int d\varepsilon_1\, d\varepsilon_2\, d\varepsilon_3\, d\varepsilon_4\, \delta(\varepsilon_1+\varepsilon_2+\varepsilon_3+\varepsilon_4) \times f(\varepsilon_1)f(\varepsilon_2)\, f(\varepsilon_3)f(\varepsilon_4)\, \sigma_n(\varepsilon_1)\sigma_{n'}(\varepsilon_1), \quad \text{(B8)}$$

$$R_2(nn') = \frac{\beta^3}{2\pi^2}\int d\varepsilon_1\, d\varepsilon_2\, d\varepsilon_3\, d\varepsilon_4\, \delta(\varepsilon_1+\varepsilon_2+\varepsilon_3+\varepsilon_4) \times f(\varepsilon_1)f(\varepsilon_2)\, f(\varepsilon_3)f(\varepsilon_4)\, \sigma_n(\varepsilon_1)\sigma_{n'}(\varepsilon_2), \quad \text{(B9)}$$

$$R_3(nn') = (-1)^{n'} R_2(nn'). \quad \text{(B10)}$$

The matrices $R_i(nn')$ are calculated in Appendix C. We shall see that they vanish if $n+n'$ is odd, i.e., the scattering matrix Q^C separates into an even and odd block. In the next section, we present closed expressions for the radial integrals $R_{1,2}$.

APPENDIX C: ENERGY INTEGRALS

The radial integral of Appendix B is given by the two basic radial integrals $R_1(nn')$ and $R_2(nn')$,

$$R_1(nn') = \frac{1}{2\pi^2}\int_{-\infty}^{\infty} dx\, f(x) I_3(x)\sigma_n(x)\sigma_{n'}(x), \quad \text{(C1)}$$

$$R_2(nn') = \frac{1}{2\pi^2}\int_{-\infty}^{\infty} dx\, dx'\, f(x)f(x') \times I_2(x+x')\sigma_n(x)\sigma_{n'}(x'), \quad \text{(C2)}$$

and $I_n(x)$ is[18]

$$I_n(x) = \int dx_1\cdots dx_n\, f(x_1)\cdots f(x_n) \times \delta(x_1+\cdots+x_n+x) \quad \text{(C3)}$$

$$= \left[1-(-1)^n\exp(-x)\right]^{-1} \frac{1}{i^{n-1}(n-1)!}\frac{\partial^{n-1}}{\partial z^{n-1}} \times \left[\left(\frac{\pi z}{\sinh \pi z}\right)^n \exp(ixz)\right]_{z=0}, \quad \text{(C4)}$$

with

$$I_2(x) = \frac{x}{1-\exp(-x)}, \quad \text{(C5a)}$$

$$I_3(x) = \frac{x^2+\pi^2}{2\,[1+\exp(-x)]}. \quad \text{(C5b)}$$

The integral $R_1(nn')$ can easily be solved with the help of the recursion of the radial basis functions σ_n, and the result is

$$R_1(nn') = \frac{(n+1)^2(n+2)^2}{4\sqrt{(2n+1)(2n+3)^2(2n+5)}}\,\delta_{n+2,n'} + \frac{n^2(n+1)^2+n^2+n-1}{2(2n-1)(2n+3)}\,\delta_{n,n'} + \frac{(n-1)^2n^2}{4\sqrt{(2n-3)(2n-1)^2(2n+1)}}\,\delta_{n-2,n'}. \quad \text{(C6)}$$

The matrix elements $R_2(nn')$, after some tedious calculations, can be expressed as complicated sums over Bernoulli numbers.[19] When we computed these matrix elements, we found the surprising result that R_2 is a banded matrix just like R_1 and its elements are given by the simple expression

$$(-1)^n R_2(nn') = \frac{(n+1)(n+2)}{2\sqrt{(2n+1)(2n+3)^2(2n+5)}}\,\delta_{n+2,n'} + \frac{n^2+n-1}{(2n-1)(2n+3)}\,\delta_{n,n'} + \frac{n(n-1)}{2\sqrt{(2n-3)(2n-1)^2(2n+1)}}\,\delta_{n-2,n'}. \quad \text{(C7)}$$

We checked the validity of Eq. (C7) for $n, n' \le 32$ on an IBM RS6000 workstation. The radial matrices $R_{1,2}$ are symmetric banded matrices and split into even and odd blocks.

[1] M. Kaveh and N. Wiser, Adv. Phys. **33**, 257 (1984).
[2] J. Bass, W. P. Pratt, and P. A. Schroeder, Rev. Mod. Phys. **62**, 645 (1990).
[3] G. R. Stewart, Rev. Mod. Phys. **56**, 755 (1984).
[4] T. R. Chien, Z. Z. Wang, and N. P. Ong, Phys. Rev. Lett. **67**, 2088 (1991).
[5] V. F. Gantmakher and Y. B. Levinson, *Carrier Scattering in Metals and Semiconductors* (North-Holland, Amsterdam, 1987).
[6] H. Smith and J. W. Wilkins, Phys. Rev. Lett. **183**, 624 (1969); H. Smith and H. Højgård Jensen, *Transport Phenomena* (Oxford University Press, Oxford, 1989).
[7] W. E. Lawrence and J. W. Wilkins, Phys. Rev. B **7**, 2317 (1973).
[8] W. W. Schulz, Ph.D. thesis, State University of New York at Stony Brook, 1993.
[9] A. H. MacDonald, Phys. Rev. Lett. **44**, 489 (1980).
[10] P. B. Allen, Phys. Rev. B **17**, 3725 (1978).
[11] J. M. Ziman, *Electrons and Phonons* (Oxford University Press, Oxford, 1960).
[12] T. Beaulac, P. B. Allen, and F. J. Pinski, Phys. Rev. B **26**, 1549 (1982).
[13] W. W. Schulz *et al.*, Phys. Rev. B **46**, 14 001 (1992).
[14] L. Lu *et al.*, Phys. Rev. Lett. **74**, 1637 (1995).
[15] B. Sanborn, P. B. Allen, and D. A. Papaconstantopoulos, Phys. Rev. B **40**, 6037 (1989).
[16] R. Askey, J. Phys. A **18**, L1017 (1985).
[17] R. Askey and J. Wilson, SIAM J. Math. Anal. **13**, 651 (1982).
[18] G. Baym and C. Pethick, in *The Physics of Liquid and Solid Helium*, edited by K. H. Bennemann and J. B. Ketterson (John Wiley and Sons, New York, 1975), Vol. 2, Chap. 1, pp. 115–117.
[19] W. W. Schulz and P. B. Allen (unpublished).